Journal of Marine Science and Engineering

MDPI

Article

Unconfined Compressive Properties of Fiber-Stabilized Coastal Cement Clay Subjected to Freeze–Thaw Cycles

Na Li [1,2], Yalan Zhu [2], Fang Zhang [2,*], Sin Mei Lim [3], Wangyi Wu [2] and Wei Wang [2]

[1] State Key Laboratory of Geomechanics and Geotechnical Engineering, Institute of Rock and Clay Mechanics, Chinese Academy of Science, Wuhan 430071, China; lina@usx.edu.cn
[2] School of Civil Engineering, Shaoxing University, Shaoxing 312000, China; zhuyalanusx@163.com (Y.Z.); wuwangyiusx@163.com (W.W.); wellswang@usx.edu.cn (W.W.)
[3] Department of Civil & Environmental Engineering, National University of Singapore, Singapore 117576, Singapore; limsinmei@nus.edu.sg
* Correspondence: zhangfang@usx.edu.cn

Abstract: This study aimed to investigate the feasibility of using polypropylene fiber-cement-stabilized coastal clay as base-course material or foundation material for city sustainable development by assessing its mechanical performance. The influence of the number of freeze–thaw cycles and curing ages on the mechanical properties of ordinary cemented clay (OCC) and polypropylene fiber-cemented clay (PCC) was investigated by using unconfined compressive test. The experimental results show that the addition of fiber with 1% content can increase the strength as well as the ductility of cemented clay by 12.5% and 15.6%, respectively. The strength of PCC and OCC at 22d age was 1.5 times than at 7d age. Under differently timed freeze–thaw cycles, the mechanical performance of PCC is improved, and, better than that, OCC improves by 11.8% in strength, 16.5% in strain and by 5% in degree of damage, indicating that fiber can improve the freeze–thaw resistance of cemented clay. The frost resistance of PCC and OCC increases with the increase in curing age. Finally, the variation of strength of OCC was explained through the change of micro-structure while the strength enhancing mechanism of polypropylene fiber for cemented clay was also revealed.

Keywords: cemented clay; freeze–thaw cycle; polypropylene fiber; unconfined compressive strength; microscopic analysis

Citation: Li, N.; Zhu, Y.; Zhang, F.; Lim, S.M.; Wu, W.; Wang, W. Unconfined Compressive Properties of Fiber Stabilized Coastal Cement-Clay Subject to Freeze-Thaw Cycles. *J. Mar. Sci. Eng.* **2021**, *9*, 143. https://doi.org/10.3390/jmse9020143

Academic Editor: Felice Rubino
Received: 4 January 2021
Accepted: 26 January 2021
Published: 30 January 2021

1. Introduction

With the rapid economic growth and continuous development of coastal cities, more and more projects are being built on soft coastal clay foundations. However, coastal clay has some disadvantages such as high natural moisture content, high compressibility and poor bearing capacity, restricting sustainable development of the coastal cities. At the same time, in cold regions, the alternation of temperature leads to the widespread distribution of seasonal permafrost, which produces a strict engineering demand for coastal clay from a frost-resistance perspective. For example, under the action of freezing, the volume expansion of soft clay with high water content will be caused by the freezing of internal water. This kind of expansion will lead to the destruction of the internal structure of the foundation clay. When the temperature gradually increases, the frozen soft clay begins to melt, resulting in the loss of part of the strength of the soft clay; as the transformation process of solid ice to liquid water advances, part of the water in the clay is gradually discharged, resulting in a large freeze–thaw settlement of the soft soil. What is more, the artificial freezing technology is sometimes used in the construction of underground engineering in the coastal soft clay area, which makes the surrounding cement clay struc-

ture experience one or more cycles of freezing and thawing, causing damage to the underground structure to a certain extent. These are serious threats to the safety of the project. Therefore, the coastal clay usually needs proper reinforcement to meet the requirement of practical engineering applications.

Cement and lime are generally adopted to promote various kinds of soil solidification, such as dredged clay [1], seashore soft clay [2], loess [3,4], coastal clay [5], subgrade clay [6] and marine clay [7]. Due to the advantages of low cost and construction feasibility, cement-treated clay is widely used in ground improvement, pavement engineering and other engineering applications [8–10]. Although the incorporation of cement can improve the clay strength to a certain extent, poor frost resistance is one disadvantage of cement-treated clay. The mechanical properties of this type of foundation change considerably under the freeze–thaw cycles with serious freeze–thaw damage, which may lead to differential settlement and instability after construction similar to nature coastal clay [11–14]. Application of cement stabilization in areas that undergo seasonal freezing has always been a major issue in engineering practice [15,16]. The freeze–thaw cycle aggravates the expansion of existing cracks in cemented clay and generates new cracks as well. Therefore, the frost resistance of different clay-based materials can be improved by delaying or decreasing the occurrence of macroscopic cracks, including overconsolidated clays [17], sulfate saline clay [18], cementitious composites [19], rubber-improved cement clay [20], and fiber-reinforced clay [21]. Recently, researchers have investigated some additives to improve the engineering performance of cement-treated clay, such as magnesium slag [22], waste tire rubber fibers [23], nano-MgO [24,25], as well as Pozzolanic [26]. On the other hand, fiber has been widely used in clay reinforcement due to its high strength, desirable frost and acid resistance, and reasonable water absorption and dispersion characteristics [27–31]. Previous studies show that the addition of fiber, such as polypropylene fiber (PPF), can effectively reduce the generation and diffusion of cracks in lime-stabilized clay [32], lime mortar [33], fly-ash-based geopolymer composites [34], cement-stabilized clay [35–37], which is an effective method for improving the frost resistance. However, the optimal amount of fiber in the coastal cement clay, as well as the improvement range of strength and the modification effect of ductility in different environments, needs further systematic research. In order to meet the requirement of the sustainable development of coastal cities, it is of great importance for people to understand properly the mechanical performance of fiber-treated cement clay under normal and freeze–thaw curing conditions.

In this study, two kinds of cement clay samples are prepared to do comparative tests to study the mechanical modification effect of fiber and evaluate the frost resistance of fiber cement clay. One is the ordinary cement clay (OCC) sample—its moisture content is 80%, the cement content is 20%. The other is polypropylene fiber-cemented clay (PCC), which is mixed with 1% polypropylene fiber on the basis of OCC. The unconfined compressive (UCS) test was used to test the mechanical properties of two kinds of cement clay. Firstly, it was carried out on two kinds of cement clay at the age of 7d, 10d, 12d, 14d, 17d and 22d to characterize the time effect of their mechanical properties. Then, it was carried out on two kinds of cement clay after different freeze–thaw cycles with an initial age of 7d to reveal the improvement effect of fiber on the freeze–thaw characteristics of cement clay. Finally, SEM micro tests were carried out on the two kinds of cement clay, and the effect of fiber on the strength mechanical properties of the cement clay was revealed from the perspective of microstructure.

2. Test Overview

2.1. Testing Materials

The testing materials used in this study are coastal soft clay, cement and polypropylene fiber. Coastal soft clay used throughout the experimental test was collected from a pit site in Zhejiang province, China. The clay was taupe in texture with an initial moisture

content of 58%, and its physical and mechanical properties are presented in Table 1. The additive, polypropylene fiber of 6 mm in length (Figure 1), was supported by Langfang Dekai Thermal Insulation Material Sales Co. Ltd, and its factory physical and mechanical parameters are shown in Table 2. The cement used belongs to class PO32.5 ordinary Portland cement. The basic properties of the cement and the clay are the same as those of the materials used in reference [5], including chemical composition, SEM picture, as well as XRD picture.

Figure 1. Polypropylene fibers.

Table 1. Physical and mechanical properties of coastal soft clay.

Wet Density ϱ /g·cm^{-3}	Moisture Content ω /%	Plastic Limit ω_P/%	Liquid Limit ω_L/%	Plasticity Index I_P	Liquidity Index I_L	Compression Coefficient α /MPa	Compression Modulus E_s/MPa
1.89	58	30	43.5	13.5	0.23	0.77	2.25

Table 2. Physical and mechanical properties of polypropylene fiber.

Specific Gravity	Diameter /μm	Length /mm	Tensile Strength /MPa	Elasticity Modulus /Mpa	Fusing Point /℃	Ignition Point /℃	Limit Tensile
0.91	18–8	6	>358	>3500	>165	590	>150%

2.2. Experimental Program

According to the results of the author's previous experiment and other scholars' research [38–40], the fiber content of this experiment is designed as 1%. The unconfined compressive (UCS) test scheme designed to investigate the effect of curing age and freeze–thaw cycles on fiber-cemented clay are summarized in Tables 3 and 4, respectively, where PPF means polypropylene fiber. In the table, the content of ingredient materials is mass percentage. At least five samples were adopted to perform each test in order to check the repeatability.

Table 3. UCS test scheme for OCC and PCC under room temperature curing.

Test Sample	Cement Content /%	Moisture Content /%	Modified Material Content /%	Curing Age /d
OCC	20	80	0	7, 10, 12, 14, 17, 22
PCC			PPF-1%	

Table 4. UCS test scheme for OCC and PCC under freeze–thaw cycle.

Test Sample	Cement Content /%	Moisture Content /%	Modified Material Content /%	Curing Age /d	Cycles of Freeze–Thaw Cycles /Number
OCC PCC	20	80	0 PPF-1%	7	3, 5, 7, 10, 15

2.3. Sample Preparation and Testing

The sample-making method was designed according to the literature reports [5] and [41]. The steps of sample preparation are stated as below:

1) The clay sample was prepared by sieving through a sieve with an aperture of 1 mm. Raw materials (cement, fiber, clay and water) were weighed based on the proposed test scheme. The initial moisture content was measured, and the water needed was calculated based on designed mix ratios. The cement content, fiber content, and water content used in preparing the sample was 20%, 1% and 80%, respectively, by percentage of dry clay weight.
2) The weighed materials were well mixed in an automatic mixing bowl and sealed with a plastic bag. In the PCC preparation, water was added two times in order to ensure the uniformity of the mix. After cement was poured into the mixing tank, half a portion of the water was then added and well mixed. The final step of mixing was followed by adding the fiber into the mix; the remaining portion of water was then added and evenly mixed to ensure homogeneity of the mixing.
3) The mixture, which was evenly mixed and then placed in a plastic bag, was then carefully squeezed into the cylindrical mold with a diameter of 39.1 mm and height of 80 mm in four layers. Manual compaction was required for each layer of clay placed into the mold by vibrating the mold twenty times by hand to ensure no trapped air was in the cement clay. This step is repeated until the mold is fully filled.
4) After flattening the excessive clay sample with an aluminum scraper, the sample was left vertically in position for approximately 30 minutes. Then, both ends of the sample were wrapped with filter paper and marked. In addition, the prepared samples were placed horizontally into a water tank for curing at room temperature and subjected to an unconfined compressive strength test on the scheduled curing day.

2.4. Freeze–Thaw Cycle Test

The test is conducted mainly according to the Chinese National Geotechnical Test Standard (GB/T 50123-1999) [42]. After curing at room temperature for 7 days, the samples were removed and wrapped with thin plastic sheet and placed in a freeze–thaw box that was subjected to 3, 5, 7, 10, and 15 freeze–thaw cycles. The freeze–thaw temperature is mainly set according to the sample material and local climate temperature. According to the literature [43], it is appropriate to set the thawing temperature of earth rock mixture as 15 °C. In reference [44], the thawing temperature of concrete is set as 20 °C. Combined with the high winter temperature of about 9 °C in Zhejiang Province, China, where the author is located, we chose positive 10 °C as the thawing temperature. The single freeze–thaw cycle was configured such that the freezing temperature and freezing time was kept constant at −10 °C and 12 h, respectively, whereas the melting temperature and melting time was also kept constant at 10 °C and 12 h, respectively. The freeze–thaw equipment is shown as Figure 2. The reference name of the sample is denoted by 7d+n, where d and n represent days and the number of freeze–thaw cycles, respectively. The samples subjected to a predetermined number of freeze–thaw cycles will then be used for the unconfined compressive strength test.

Figure 2. The freeze–thaw equipment.

3. Test Results and Analysis

Unconfined compressive strength is an important mechanical parameter in practical engineering construction. When determining the unconfined compressive strength, the axial stress at the peak point is taken as the value of the peak value occurs in a stress–strain curve; meanwhile the axial stress is taken at an axial strain of 15% when the peak reaches plateau with a less obvious peak being observed.

3.1. The Influence of Curing Age

Figure 3 reflects the stress–strain relationship of OCC and PCC after curing at room temperature for 7, 10, 12, 14, 17, and 22 days. It can be seen from Fig. 3 that the shape of the stress–strain curves at each age are quite similar, and the development of the trend for each individual curve before and after the peak point is basically the same for all the samples. This specific behavior is observed by considering that (1) all the curves passed the coordinates of the origin; (2) with the increase in strain, the stress increases continuously in a convex manner before reaching the peak point; after the peak point, the stress first decreases convexly, then concavely, and finally becomes flat or constant.

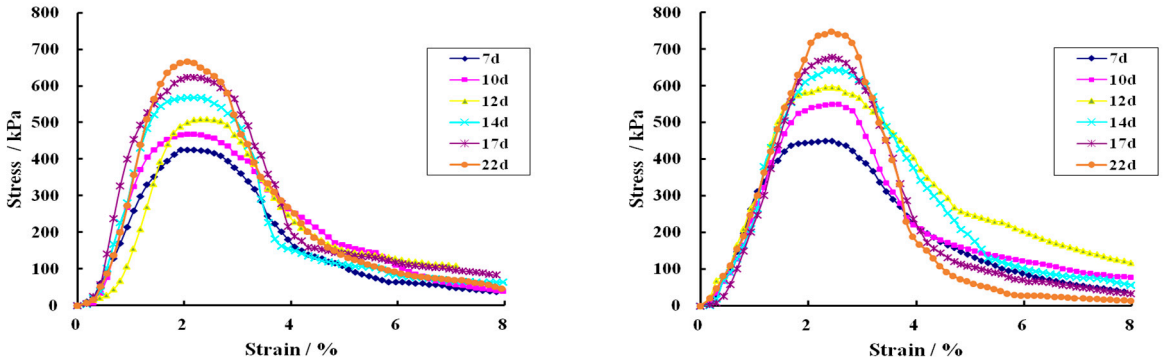

Figure 3. Stress–strain curves of OCC and PCC at room temperature. (**a**) Ordinary coastal cement clay (OCC); (**b**) polypropylene fiber-cemented clay (PCC).

The peak value of the stress–strain curve is taken as the UCS of the corresponding sample. It can be seen from Tables 5 and 6 that the UCS of OCC and PCC gradually increases with the increase in curing age. Generally, the strength of PCC and OCC at 22d age is 1.5 times that at 7d age. For OCC, the strength increases by 39 kPa from 7 days to 10 days, 157 kPa from 10 days to 17 days, while 45 kPa from 17 days to 22 days. Similarly,

for PCC: the strength increases by 96 kPa from 7 days to 10 days, 142 kPa from 10d to 17d, while 43 kPa from 17 days to 22 days. It can be seen that the equivalent increment amount in unconfined compressive strength for both OCC and PCC is almost consistent with the curing age. It can also be found that the unconfined compressive strength of PCC is about 12.5% higher than that of OCC, which means the addition of fiber increases the strength of cemented clay.

At the same time, Tables 5 and 6 demonstrate that the axial strain corresponding to OCC failure is approximately 2.1%, while that of PCC is approximately 2.4% with an average increase of about 15.6. This indicates that the presence of PPF in the cemented clay not only can improve its unconfined compressive strength but also have the potential in increasing the ductility of the cemented clay. From the above phenomenon observed, it is obvious that the mechanical performance of PCC is much better than that of OCC. This can be attributed to the physical properties of fiber: when stress is being applied on PCC, the fiber is pulled due to the displacement of clay and cement mineral particles, which can increase the sample's ductility.

Table 5. UCS and strain of OCC at failure point.

Curing Age /d	7	10	12	14	17	22
UCS /kPa	425	464	509	565	621	666
Strain /%	2.06	2.07	2.11	2.06	2.07	2.18

Table 6. Peak UCS and strain of PCC at failure point.

Curing Age/d	7	10	12	14	17	22
UCS /kPa	450	546	592	646	688	731
Strain /%	2.31	2.44	2.44	2.44	2.44	2.44

3.2. The Influence of Freeze–Thaw Cycles

In order to study the influence of freeze–thaw cycles on the strength properties of OCC and PCC, the stress–strain curves of samples with 7d curing age subjected under various freeze–thaw cycles were shown in Figure 4. In Figure 4, 7d refers to the curing age of the specimen at the beginning of freeze–thaw, and the number after the plus sign refers to the number of freeze–thaw cycles of the specimen after 7d curing. For example, 7d+3 means that the specimen is cured for 7d and then subjected to three freeze–thaw cycles.

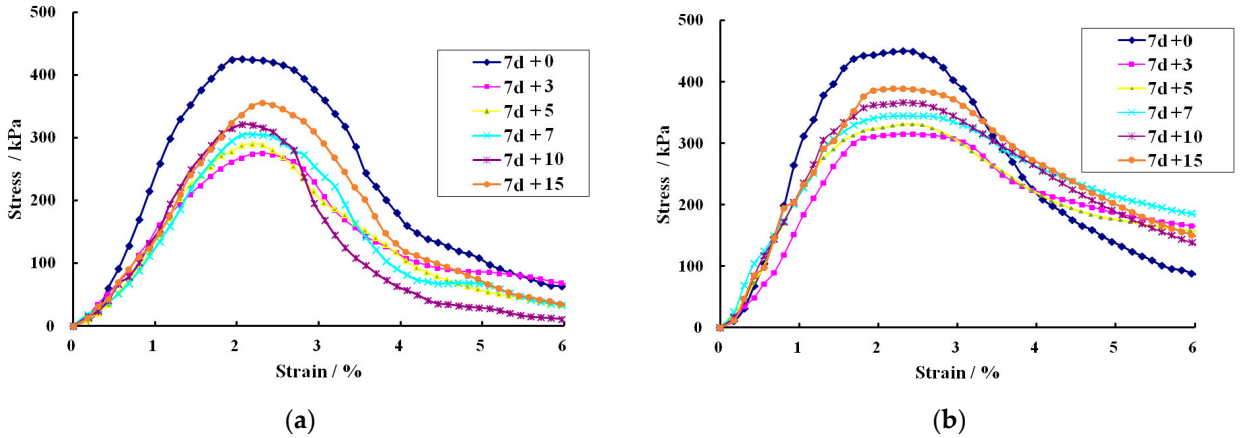

Figure 4. Stress–strain curves of OCC and PCC under freeze–thaw cycles. (**a**) Ordinary coastal cement clay (OCC); (**b**) polypropylene fiber coastal cement clay (PCC).

It can be seen from Fig. 4 that the stress–strain curves of OCC and PCC show obvious strain-softening behavior. For OCC, the stress–strain curve reaches its peak strength when the axial strain is approximately 2%; while for PCC, it reaches peak strength at the axial strain between 2% and 3%. In the first few freeze–thaw cycles, the stress–strain curves show a drastic downward shift, especially for the third cycle. The possible reason is that during the freeze–thaw cycle, frost heaving and thawing in the clay will create larger pores between the clay particles.

It is evident in Figure 5 that the unconfined compressive strength of PCC is about 11.8% higher than that of OCC after undergoing several freeze–thaw cycles. This indicates that fiber can increase the clay strength under freeze–thaw cycle as well as improving the frost resistance of OCC unreservedly. There is a drastic decrease in the unconfined compressive strength from 0 to 3 cycles, and a decrease gradually as the number of freeze–thaw cycles increases. This implies that the initial three freeze–thaw cycles contribute the most to the damage of the clay. The unconfined compressive strengths of the OCC samples subjected under 3, 5, 7, 10, and 15 freeze–thaw cycles were 275 kPa, 290 kPa, 305 kPa, 322 kPa, and 355 kPa, respectively. The strength reached the peak when the axial strain was about 2.08%, whereas the unconfined compressive strengths of PCC samples were 315 kPa, 330 kPa, 345 kPa, 366 kPa, and 389 kPa, respectively; the strengths reached their peak when the axial strain was averaging at 2.42% with almost 16.5% increase.

As the sample went through the process of freeze–thaw cycles, its curing age also increased which led to an increase in the hydration products. It is noted that as the samples were subjected to 15 freeze–thaw cycles, the cement hydration reaction lasted for 22 days, leading to an increase in both the compressive strength and frost resistance. Therefore, Figure 5 illustrates a trend of slight growth in the later stage and finally reaches plateau at the end of the freeze–thaw cycles. It was also observed that a sharp declination of the strength of cemented clay in the early stage as the samples were subjugated by the damage incurred when the samples were subjected to freeze–thaw cycle ahead of the hydration reaction by the cement.

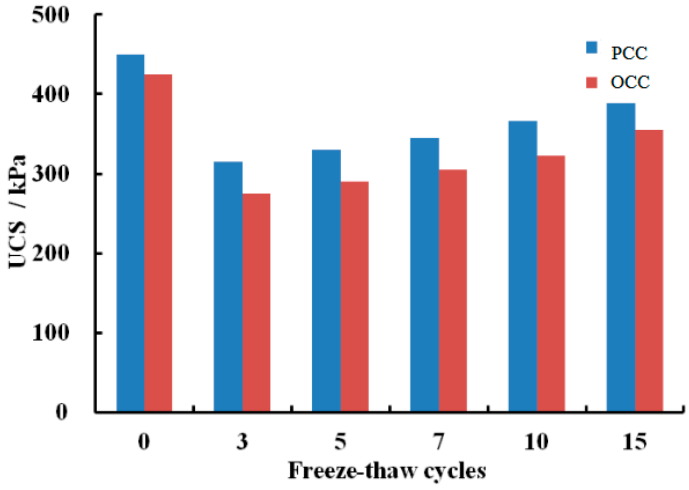

Figure 5. Influence of freeze–thaw cycles on unconfined compressive strength.

3.3. The Degree of Damage

In order to analyze the influence of freeze–thaw cycles on the unconfined compressive strength of OCC and PCC, the degree of damage due to freeze–thaw, D is suggested [45] as formula (1):

$$D = \left(1-\frac{q_n}{q_0}\right)\times 100\% \quad (1)$$

where D = degree of damage;

q_n = unconfined compressive strength after n cycles of freeze–thaw;

q_0 = unconfined compressive strength without subjecting to freeze–thaw cycle.

Based on the above formula, the degree of damage under various freeze–thaw cycles for PCC and OCC was calculated and presented in Figure 6. It can be observed that the degree of damage of PCC is significantly lower than that of OCC, indicating that the greater the degree of damage, the lower the compressive strength of the clay. The freeze–thaw damage of PCC with fiber addition was about 5% lower than that of OCC, indicating that PCC has the ability to resist freeze–thaw cycles. During the zeroth to third freeze–thaw cycle, the sample damaged very quickly, which led to a steep increase in the degree of damage, signifying consequential degradation of the clay within this cycle. Right after the third freeze–thaw cycle, a decreasing trend was observed to be quite linearly over the time as the corresponding compressive strength rises progressively. This is because there are more pores developed at the beginning of the freeze–thaw cycles, which then gradually become more stable over the freeze–thaw cycles. Meanwhile, as the number of freeze–thaw cycles increases over time, the process of hydration in cement continues to take place while improving the clay strength, which assists in resisting some degree of damage [46].

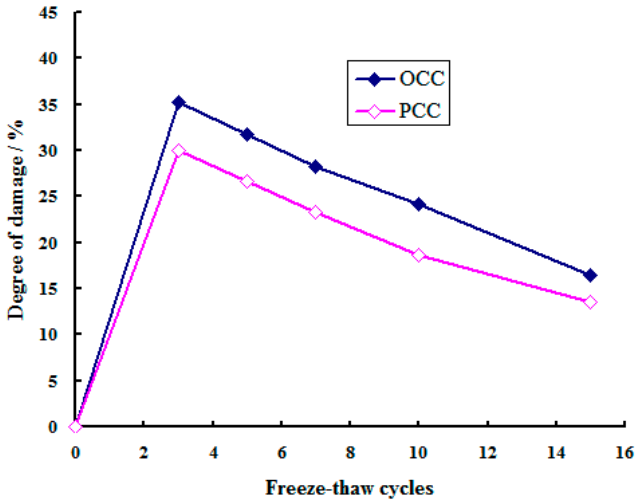

Figure 6. The influence of number of freeze–thaw cycles on the degree of damage.

3.4. Failure Mode of Cemented Clay

Figure 7 shows the failure pattern of the OCC sample subjected to axial load under different freeze–thaw cycles. When the number of freeze–thaw cycle increases, the damage of the sample is more significant based on the visual observation. As shown in Figure 7a for the zero freeze–thaw cycle, some small visible vertical cracks at the bottom of the sample can be seen, while the development of the crack does not run through the whole sample. With the increase in freeze–thaw cycles (three or five cycles), the damage of the sample is more obvious and many evident cracks appear through the sample, as shown in Figure 7b. After being subjected to more freeze–thaw cycles (7, 10 or 15 cycles), some huge cracks can be easily identified when the sample fails, as presented in Figure 7c.

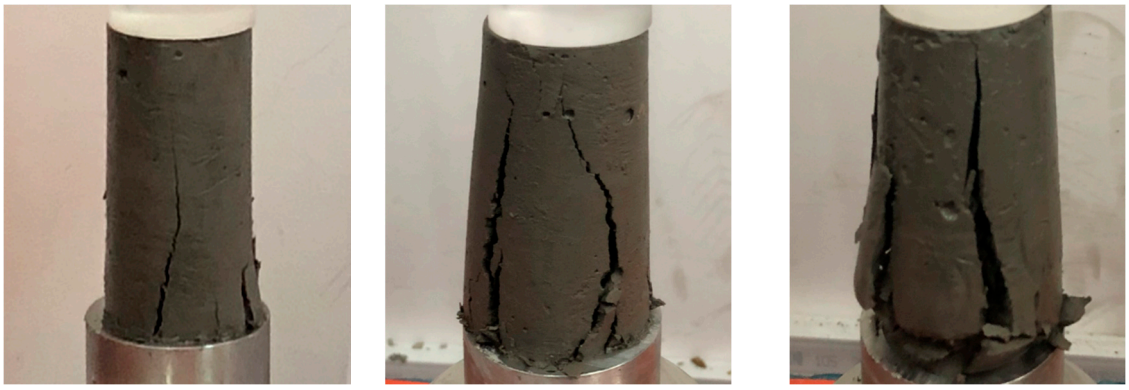

(a) (b) (c)

Figure 7. Failure pattern of OCC after UCS test under various freeze–thaw cycles. (**a**) 0 cycle; (**b**) 5 cycles; (**c**) 15 cycles.

The failure patterns of PCC corresponding to different freeze–thaw cycles are shown in Figure 8. It can be seen that the addition of polypropylene fiber leads to obvious slantwise cracks in the sample. For the zero freeze–thaw cycle, it is illustrated in Figure 8a that there is only one gentle inclined crack. After being subjected to more freeze–thaw cycles, it can be clearly seen from Figure 8b that there is chap appearing on the sample surface, and an obvious diagonal crack when the sample fails. For the sample subjected to 10 and 15 (Figure 8c) freeze–thaw cycles, some fibers are exposed as the sample fails. However, there is still some connection between the fiber and cemented clay lump.

(a) (b) (c)

Figure 8. Failure pattern of PCC after UCC test under various freeze–thaw cycles. (**a**) 0 cycle; (**b**) 5 cycles; (**c**) 15 cycles.

Comparing the failure pattern of OCC and PCC, it can be seen that the bonding of OCC sample is not as desirable as that of PCC. For OCC, the samples tend to break into pieces after destruction, with no significant adherence observed. For PCC, the addition of fiber is able to form a spatial network structure since PPFs are randomly distributed inside the sample. When PCC is under a static vertical load, the fiber could effectively prevent further development of cracks, and the occurrence of the brittle fracture of the sample. In addition, the fiber also absorbs part of the energy, delaying the expansion of cracks and avoiding spalling of sample after destruction. This phenomenon can be clearly observed from the sectional view of the sample after failure shown in Figure 9. Overall, the above findings indicate that the addition of polypropylene fiber could improve the internal connection of the sample, which is beneficial to the freeze–thaw resistance.

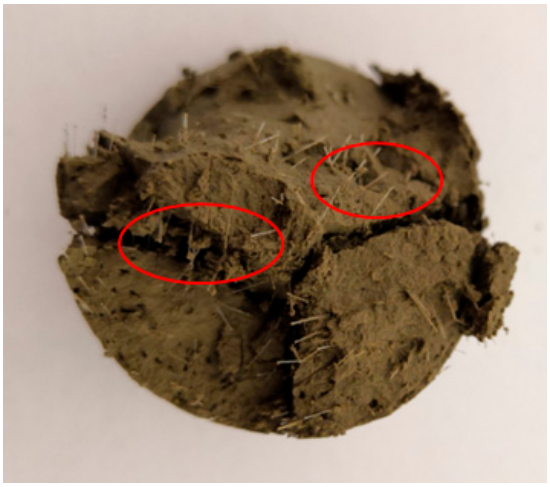

Figure 9. Sectional view of PCC after failure.

4. Microscopic Analysis

Scanning electron microscope (SEM) is conducted to investigate the micro-structure of OCC and PCC under various freeze–thaw cycles, as shown in Figure 10. In this figure, the square denotes the pores; the oval denotes hydration products with flake or needle.

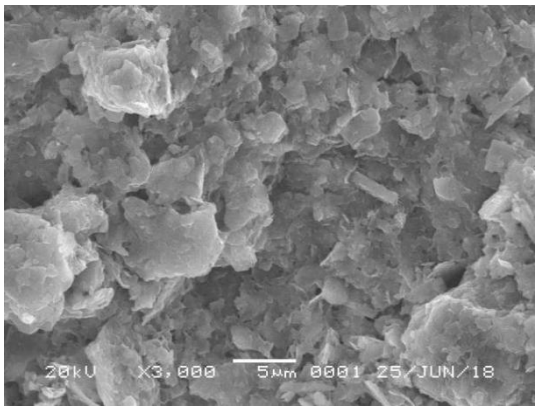

(**a-1**)

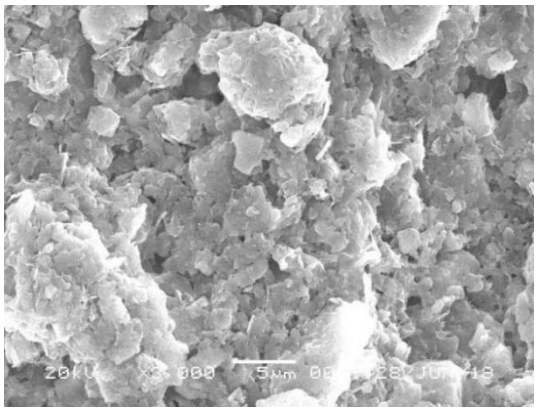

(**a-2**)

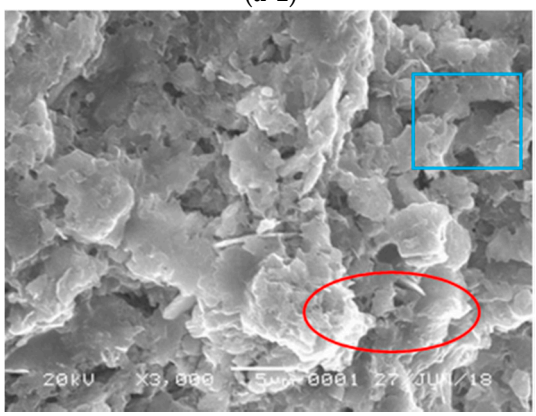

(**b-1**)

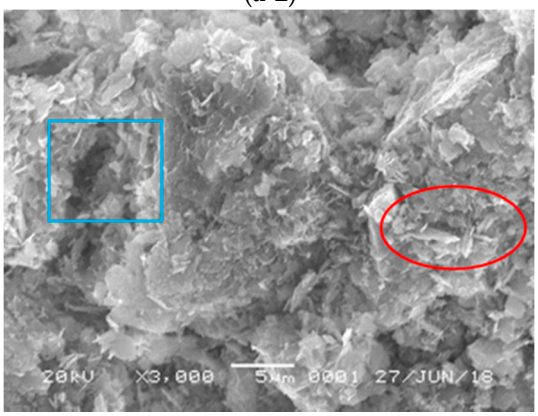

(**b-2**)

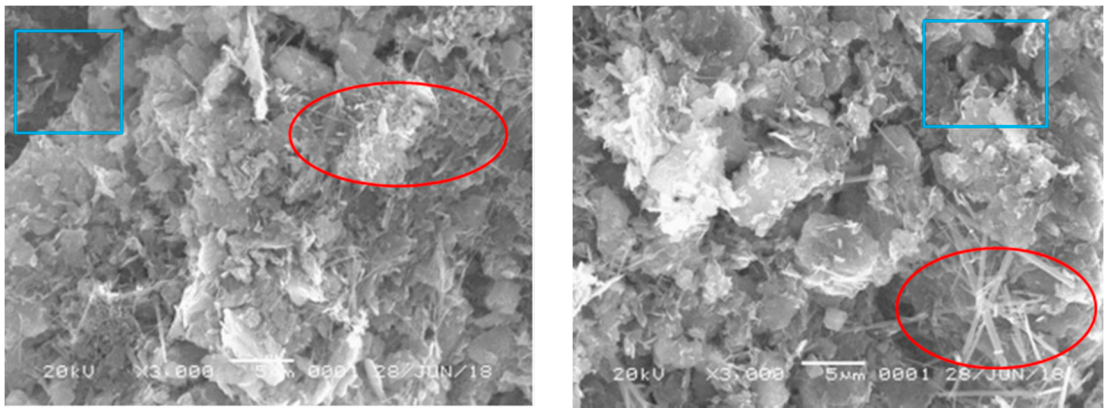

(**c-1**) (**c-2**)

Figure 10. SEM image. (**a-1**) OCC; (**a-2**) PCC; (**b-1**) OCC under 3 freeze–thaw cycles; (**b-2**) PCC under 3 freeze–thaw cycles; (**c-1**) OCC under 15 freeze–thaw cycles; (**c-2**) PCC under 15 freeze–thaw cycles.

As illustrated in Figure 10a-1, there are some obvious pores inside the OCC sample. This is primarily due to the incomplete hydration of cement. When the sample undergoes the third freeze–thaw cycle, as its corresponding age is also increased by three days, the hydration reaction tends to be more complete than that of 7d. It can be seen from the SEM image in Figure 10b-1 that some acicular hydration products are distributed in the clay. After 15 freeze–thaw cycles, as shown in Figure 10c-1, the hydration reaction is seen to be almost complete, and the hydration products with flake and needle shapes fill the pores in the clay sample. Moreover, these hydrated crystals have high strength and cohesiveness, forming a flocculated network structure, which firmly binds the clay particles together. At the same time, during the freeze–thaw cycle, the sample was first left above 0 °C for a period of time, thus making the frost on the clay surface melt into water droplets. The water then permeated into the structure along the pores or capillary pores on the structure's surface. When the temperature drops below 0 °C, crack formation occurs as a result of the freezing and expansion of water.

Figure 10a-2, b-2 and c-2 show the micro-structure for PCC. A similar observation could be achieved that can be compared with that of OCC. The needle-like crystals of the hydrates are bound into a network structure, which greatly improves the bonding strength between the fibers and cemented clay. This restricts the relative sliding of fibers. It can also be seen from Figure 11 that PPF is distributed in a disorderly manner in cemented clay. When subjected to an external force, it will produce high friction between the fiber and the cemented clay. As the cracks occurred when the sample was subjected to an axial static load, it required a certain amount of effort for the fiber to be pulled out, which is the strength enhancing mechanism.

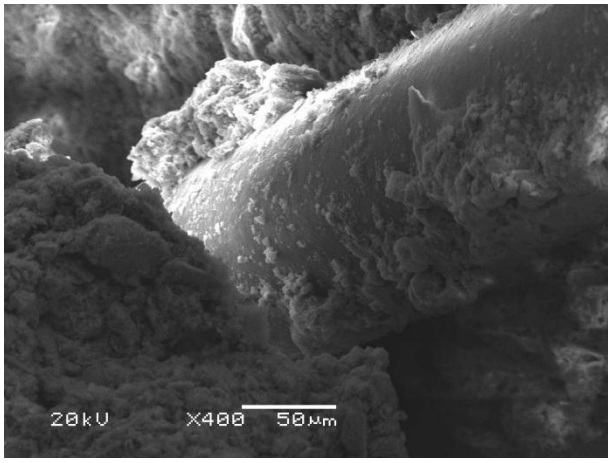

Figure 11. Shape of fiber in the clay.

5. Conclusions and Discussions

5.1. Conclusions

In this study, unconfined compressive strength tests were carried out on OCC and PCC samples to investigate the effect of freeze–thaw cycles. Based on the test data, the stress–strain relationship is analyzed, and the mechanical properties of the cemented clays are investigated. Finally, a SEM test was also carried out to analyze the micro-structure of cemented clay. The following conclusions could be drawn: The strength of both OCC and PCC increases with the curing age, and the growth rate is roughly equivalent. The compressive strength of PCC is always greater than that of OCC under both normal curing condition and freeze–thaw cycles, while the addition of fiber also increases the failure strain of cemented clay. Freeze–thaw cycle has an adverse effect on the strength of cemented clay, which is obvious in the early stage. As the number of freeze–thaw cycles increases, the degradation effect of freeze–thaw cycle begins to reduce due to the generation of hydration products. Under freeze–thaw cycles, the strength of two kinds of cement samples first decreases and then increases slowly. The hydration product covers the fiber surface, which effectively limits the relative sliding of the fiber in the cemented clay and improves the ability to resist frost damage. The results of this study may provide a foundation for coastal clay-treated engineering design for sustainable planning of cities experiencing freeze–thaw seasons.

5.2. Discussions

The test results of this paper are similar to those of Wang [6] and Orakoglu [13], both of which show that the fiber has a better improvement effect on cement clay, both in terms of unconfined compressive strength and tensile properties. This paper emphasizes the time effect and freeze–thaw effect of fiber on the modification effect of cement clay.

It should be noted that, although the polypropylene fiber is conducive to improving the unconfined compressive properties of cement stabilized coastal clay, there are two limitations in this study. First, the mechanical test method is relatively simple, only considering the unconfined compression test. Other methods such as conventional triaxial test, splitting tensile test, small strain test, dynamic triaxial test and consolidation test need to be further studied. The second is that the starting freezing and thawing age of samples is single, only 7 days are considered. In order to meet the needs of practical engineering, it is necessary to further test the samples with starting freezing and thawing of 28d and 60d age.

Fiber-modified cement clay is a special material mixed with fiber, cement, coastal soft clay and water, which has complex chemical composition. Under complex conditions,

such as normal maintenance and freeze–thaw cycle, the process of strength development and internal structure change may be accompanied by complex phase transformation [47,48]. It is a new idea to study the mechanical properties of fiber-reinforced cement clay with phase transformation theory.

Author Contributions: All authors contributed substantially to this study. Individual contributions were writing—review and editing, N.L. and F.Z.; investigation, Y.Z. and W.W. (Wangyi Wu); validation, S.M.L. and W.W. (Wei Wang). All authors have read and agreed to the published version of the manuscript.

Funding: This research was funded by the Open Research Fund of State Key Laboratory of Geomechanics and Geotechnical Engineering, Institute of Rock and Clay Mechanics, Chinese Academy of Science (grant number Z017013), and the Zhejiang Provincial Natural Science Foundation of China (grant number LY17E080016)

Institutional Review Board Statement: Not applicable.

Informed Consent Statement: Not applicable.

Data Availability Statement: The data presented in this study are available on request from the corresponding author.

Conflicts of Interest: The authors declare no conflict of interest.

References

1. Jan, O.Q.; Mir, B.A. Strength behaviour of cement stabilised dredged clay. *Int. J. Geosynth. Ground Eng.* **2018**, *4*, 4–16.
2. Wang, W.; Zhang, C.; Li, N.; Tao, F.F. Characterisation of nano magnesia-cement-reinforced seashore soft clay by direct-shear test. *Marine Georesources Geotechnol.* **2019**, *37*, 989–998.
3. Jia, L.; Guo, J.; Jiang, Y.B.; Fu, Y.; Zhou, Z.D.; Lim, S.M.; Zhao, X.S. Experimental investigation on shear strength parameters of lime stabilized loess. *Sustainability* **2019**, *11*, 5397.
4. Jia, L.; Zhang, L.; Guo, J.; Yao, K.; Lim, S.M.; Li, B.; Xu, H. Evaluation on strength properties of lime-slag stabilized loess as pavement base material. *Sustainability* **2019**, *11*, 4099.
5. Li, N.; Zhu, Q.Y.; Wang, W.; Song, F.; An, D.L.; Yan, H.R. Compression characteristics and microscopic mechanism of coastal clay modified with cement and fly ash. *Materials* **2019**, *12*, 3182.
6. Wang, W.; Zhang, C.; Guo, J.; Li, N.; Li, Y.; Zhou, Z.; Liu, Y. Investigation on the triaxial mechanical characteristics of cement-treated subgrade clay admixed with polypropylene fiber. *Appl. Sci.* **2019**, *9*, 4557.
7. Khoshsirat, V.; Bayesteh, H.; Sharifi, M. Effect of high salinity in grout on the performance of cement-stabilized marine clay. *Constr. Build. Mater.* **2019**, *217*, 93–107.
8. Mollamahmutoglu, M.; Avcı, E. Cement type effect on improvement of clayey clay properties. *ACI Mater. J.* **2018**, *115*, 855–866.
9. Yao, K.; Li, N.; Chen, D.H.; Wang, W. Generalized hyperbolic formula capturing curing period effect on strength and stiffness of cemented clay. *Constr. Build. Mater.* **2019**, *199*, 63–71.
10. Gao, L.; Ren, Z.; Yu, X. Experimental study of nanometer magnesium oxide-modified clay. *Mech. Found. Eng.* **2015**, *52*, 218–224.
11. Wang, W.; Li, Y.; Yao, K.; Li, N.; Zhou, A.Z.; Zhang, C. Strength properties of nano-MgO and cement stabilized coastal silty clay subjected to sulfuric acid attack. *Marine Georesources Geotechnol.* **2020**, *38(10)*, 1177–1186.
12. Tebaldi, G.; Orazi, M.; Orazi, U.S. Effect of freeze-thaw cycles on mechanical behavior of lime-stabilized clay. *J. Mater. Civil Eng.* **2016**, *28*, 06016002.
13. Orakoglu, M.E.; Liu, J. Effect of freeze-thaw cycles on triaxial strength properties of fiber-reinforced clayey clay. *KSCE J. Civil Eng.* **2017**, *21*, 2128–2140.
14. Kumar, A.; Soni, D.K. Study of the mechanical behaviour of a clayey clay under normal and frozen conditions. *Slovak J. Civil Eng.* **2019**, *27*, 29–35.
15. Tajdini, M.; Bonab, M.H.; Golmohamadi, S. An experimental investigation on effect of adding natural and synthetic fibres on mechanical and behavioural parameters of clay–cement materials. *Int. J. Civil Eng.* **2018**, *16*, 353–370.
16. Xu, J.; Ren, J.; Wang, Z.; Wang, S.; Yuan, J. Strength behaviors and meso-structural characters of loess after freeze-thaw. *Cold Reg. Sci. Technol.* **2018**, *148*, 104–120.
17. Ji, L.Q.; Wei, M.A. Influence of freezing-thawing on strength of overconsolidated clays. *Chin. J. Geotech. Eng.* **2006**, *28*, 2082–2086.
18. Zhang, W.; Ma, J.; Tang, L. Experimental study on shear strength characteristics of sulfate saline clay in Ningxia region under long-term freeze-thaw cycles. *Cold Reg. Sci. Technol.* **2019**, *160*, 48–57.
19. Zhong, J.; Shi, J.; Shen, J.; Zhou, G.; Wang, Z. Investigation on the failure behavior of engineered cementitious composites under freeze-thaw cycles. *Materials* **2019**, *12*, 1808.

20. Wang, F.; Ping, X.; Zhou, J.; Kang, T. Effects of crumb rubber on the frost resistance of cement-clay. *Constr. Build. Mater.* **2019**, *223*, 120–132.
21. Kravchenko, E.; Liu, J.; Niu, W.; Zhang, S. Performance of clay reinforced with fibers subjected to freeze-thaw cycles. *Cold Reg. Sci. Technol.* **2018**, *153*, 18–24.
22. Amini, O.; Ghasemi, M. Laboratory study of the effects of using magnesium slag on the geotechnical properties of cement stabilized clay. *Constr. Build. Mater.* **2019**, *223*, 409–420.
23. Bekhiti, M.; Trouzine, H.; Rabehi, M. Influence of waste tire rubber fibers on swelling behavior, unconfined compressive strength and ductility of cement stabilized bentonite clay clay. *Constr. Building Mater.* **2019**, *208*, 304–313.
24. Yao, K.; An, D.; Wang, W.; Li, N.; Zhang, C.; Zhou, A.Z. Effect of nano-MgO on mechanical performance of cement stabilized silty clay. *Marine Georesources Geotechnol.* **2020**, *38(2)*, 250–255.
25. Yao, K.; Wang, W.; Li, N.; Zhang, C.; Wang, L.X. Investigation on strength and microstructure characteristics of nano-MgO admixed with cemented soft clay. *Constr. Build. Mater.* **2019**, *206*, 160–168.
26. Ouhadi, V.R.; Yong, R.N.; Amiri, M. Pozzolanic consolidation of stabilized soft clays. *Appl. Clay Sci.* **2014**, *95*, 111–118.
27. Zaimoglu, A.S.; Tan, O.; Akbulut. R.K. Optimization of consistency limits and plasticity index of fine-grained clays modified with polypropylene fibers and additive materials. *KSCE J. Civil Eng.* **2016**, *20*, 662–669.
28. Mahrous, M.A.; Segvic, B.; Zanoni, G.; Khadka, S.D.; Senadheera, S.; Jayawickrama, P.W. The role of clay swelling and mineral neoformation in the stabilization of high plasticity soils treated with the fly ash- and metakaolin-based geopolymers. *Minerals* **2018**, *8*, 146.
29. Consoli, N.C.; Bassani, M.A.A.; Festugato, L. Effect of fiber-reinforcement on the strength of cemented clays. *Geotext. Geomembr.* **2010**, *28*, 344–351.
30. Jiang, P.; Mao, T.; Li, N.; Jia, L.; Zhang, F.; Wang, W. Characterization of short-term strength properties of fiber/cement-modified slurry. *Adv. Civil Eng.* **2019**, 3789403, doi:10.1155/2019/3789403.
31. Hamidi, A.; Hooresfand, M. Effect of fiber reinforcement on triaxial shear behavior of cement treated sand. *Geotext. Geomembr.* **2013**, *36*, 1–9.
32. Boz, A.; Sezer, A. Influence of fiber type and content on freeze-thaw resistance of fiber reinforced lime stabilized clay. *Cold Reg. Sci. Technol.* **2018**, *151*, 359–366.
33. Benchiheub, D.; Amouri, C.; Houari, H.; Belachia, M. Effect of natural pozzolana and polypropylene fibers on the performance of lime mortar for old buildings restoration. *J. Adhes. Sci. Technol.* **2018**, *32*, 1324–1340.
34. Al-mashhadani, M.M.; Canpolat, O.; Aygörmez, Y.; Uysal, M.; Erdem, S. Mechanical and microstructural characterization of fiber reinforced fly ash based geopolymer composites. *Constr. Building Mater.* **2018**, *167*, 505–513.
35. Ding, M.; Zhang, F.; Ling, X.; Lin, B. Effects of freeze-thaw cycles on mechanical properties of polypropylene fiber and cement stabilized clay. *Cold Regions Science and Technology*, **2018**, *154*, 155–165.
36. Orakoglu, M.E.; Liu, J.; Niu, F. Dynamic behavior of fiber-reinforced clay under freeze-thaw cycles. *Clay Dyn. Earthq. Eng.* **2017**, *101*, 269–284.
37. Chaduvula, U.; Desai, A.K.; Solanki, C.H. Application of triangular polypropylene fibres on clay subjected to freeze–thaw cycles. *Indian Geotech. J.* **2014**, *44*, 351–356.
38. Tran, K.Q.; Satomi, T.; Takahashi, H. Improvement of mechanical behavior of cemented soil reinforced with waste cornsilk fibers. *Constr. Build. Mater.* **2018**, *178*, 204–210.
39. Yang, B.H.; Weng, X.Z.; Liu, J.Z.; Kou, Y.N.; Jiang, L.; Li, H.L.; Yan, X.C. Strength characteristics of modified polypropylene fiber and cement-reinforced loess. *J. Cent. South Univ.* **2017**, *24*, 560–568.
40. Hu, W.L.; He, P.L.; Liu, H. Experimental study on optimization of shear strength parameters of basalt fiber loess. *Chinese J. Geol. Hazard Control* **2019**, *30*, 92–97.
41. Chen, Q.Q.; Yao, K.; Liu, Y. Stress-dependent behavior of marine clay admixed with fly-ash-blended cement. *Int. J. Pavement Res. Technol.* **2018**, *11*, 611–616.
42. *Chinese National Geotechnical Test Standard*; GB/T 50123-1999; Code of China: Peking, China, 1999.
43. Zhou, Z.; Xing, K.; Yang, H.; Wang, H. Damage mechanism of soil-rock mixture after freeze-thaw cycles. *J. Cent. South Univ.* **2019**, *26*, 13–24.
44. Dai, M.X.; Zhang, C.K.; He, Y.L.; Fang, L.Q.; Han, C.P. Shear strength analysis of polypropylene fiber soil under freeze-thaw cycles. *Constr. Technol.* **2018**, *47*, 1125–1130.
45. He, M.M. *Experimental Study on Mechanical Properties of Fiber Loess under Freeze-Thaw Cycles*; Xi'an University of Technology: Xi'an, China, 2019; Volume 1.
46. Wu, W.Y. *UCS Experiment and Microscopic Mechanism of Modified Seashore Soft Soil under Freeze-Thaw Environment*; Shaoxing University: Shaoxing, China, 2019; Volume 3.
47. Roy, A.M. Effects of interfacial stress in phase field approach for martensitic phase transformation in NiAl shape memory alloys. *Appl. Phys. A* **2020**, *126*, 576.
48. Arunabha, M.R. Influence of Interfacial Stress on Microstructural Evolution in NiAl Alloys. *JETP Lett.* **2020**, *112*, 173–179.